Sensors & Actuators: A. Physical 362 (2023) 114632

Contents lists available at ScienceDirect

Sensors and Actuators: A. Physical

journal homepage: www.journals.elsevier.com/sensors-and-actuators-a-physical

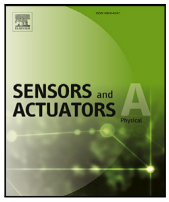

Water vapor concentration measurements in high purity gases by means of comb assisted cavity ring down spectroscopy

Eugenio Fasci [a,*], Muhammad Asad Khan [a], Vittorio D'Agostino [a], Stefania Gravina [a], Vito Fernicola [b], Livio Gianfrani [a], Antonio Castrillo [a]

[a] Dipartimento di Matematica e Fisica Università degli Studi della Campania "Luigi Vanvitelli", Viale Lincoln, 5, Caserta, 81100, Italy
[b] Istituto Nazionale di Ricerca Metrologica (INRIM), Strada delle Cacce, 91, Torino, 10135, Italy

ARTICLE INFO

Keywords:
Cavity ring-down spectroscopy
High-sensitivity
Water mole fraction
Optical frequency comb synthesizer
Part per trillion

ABSTRACT

In manufacturing processes of semiconductor industry accurate detection and monitoring of water vapor concentration in trace amount is of great importance. The ability to perform reliable measurements in ultra-pure gases, with a wide dynamic range and low uncertainty, can have a substantial impact on product quality and process performances. Here, we report on the development of a second-generation comb-assisted cavity ring-down spectrometer and present H_2O mole fraction measurements in high-purity N_2 gas. Based on the use of a pair of phase-locked lasers and referenced to an optical frequency comb synthesizer, the spectrometer allowed to record high-quality absorption spectra in coincidence with the $3_{2,2} \rightarrow 2_{2,1}$ H_2O transition at 1.3946 μm. Retrieval of water mole fractions, at levels as low as 380 part per billion, was accomplished through a careful spectra analysis procedure based on the use of refined line shape models which include speed-dependent effects. Measurements were performed with a statistical reproducibility of 5 parts per billion, for an integration time of about 0.2 s. The noise equivalent and minimum detectable absorption coefficients were found to be 3.1×10^{-11} $cm^{-1}/\sqrt{Hz}$ and 6.5×10^{-12} cm^{-1}, respectively. This latter allowed for a minimum detectable water mole fraction (limit of detection) of 160 parts per trillion. Finally, the main sources of systematic uncertainty have been discussed and quantified.

1. Introduction

For humans, water represents the most important substance without which life would not be possible. Nevertheless, in some cases, its presence becomes a serious issue that is not easily to be overcome. Residual water content (often referred to as moisture) in some scientific contexts can jeopardize the success of well-designed experiments. Just to cite an example, in gravitational wave detection experiments, the phase noise due to residual water content in the vacuum tubes is not a limiting factor provided that water pressure is kept below the level of 10^{-8} Pa [1]. Not less important is the role that water plays in some industry sectors, with a particular accent for semiconductor manufacturing where high-vacuum conditions and/or high-purity gases are absolutely required. In fact, water is considered one of the most significant contaminants during fabrication processes because it can adversely affect the efficiency as well as the noise performances of semiconductor materials. Its detrimental effect on the optoelectronic properties of the final devices is further amplified by the fact that water is present in the atmosphere in large quantities, and, therefore, it spreads readily everywhere. Moreover, due to its chemical properties, it sticks on any metallic surface becoming the most difficult impurity to remove. For all reasons stated above, the precise, highly sensitive, and real-time monitoring of water content has become an increasing demand from both the scientific community and the industry [2]. For example, in the case of high-purity nitrogen gas, used to prevent contamination of the semiconductor wafer surface, the admitted levels of residual water are below 100 parts per-billion (ppb) [3]. Other interesting cases are represented by the fabrication of light emitting diodes, laser devices, and solar cells where the specifications in terms of residual water mole fraction are even more stringent [4]. In exacerbating these demands, it could be noted that problems related to moisture are not simply avoided by purchasing the highest quality gas source. Each element in a gas distribution system potentially can be a source of contamination due to the polar nature of the molecule. This circumstance enhances the need of control and measuring water vapor concentrations even up to mole fractions near the ppb level. Many types of methods and instruments have been developed for moisture determinations over the years, including atmospheric-pressure ionization

* Corresponding author.
E-mail address: eugenio.fasci@unicampania.it (E. Fasci).

https://doi.org/10.1016/j.sna.2023.114632
Received 30 May 2023; Received in revised form 4 August 2023; Accepted 30 August 2023
Available online 9 September 2023

mass spectrometry [5], chilled-mirror hygrometers [6], electrolytic sensors [7], oscillating quartz crystal mechanical microbalances [8], and capacitance sensors [9]. Shortcomings of these approaches include high costs, slow response times, poorly characterized surface interactions, indirect calibration, or inability to measure moisture in hydrogen, oxygen, and condensable or corrosive gases. More recently, miniaturized solutions, based on solid-state sensing films that interact with water vapor and convert the concentration into an electrical signal, have been proposed [10]. However, also these sensors have some drawbacks, such as drifts and contamination-induced inaccuracies. As proof of the relevance of these issues, in 2016, on-chip photonic micro-ring resonators, supporting high-Q whispering gallery modes, have been developed as integrated photonic moisture sensors [11].

Despite the enormous demand of capability of detecting very low water concentrations, the available instruments reported above are often limited by large uncertainties and low detection limits. In this respect, spectroscopic methods can be considered a valuable alternative. These techniques not only offer high sensitivities and fast response times but are also easily adapted for online monitoring applications. Further, they can be applied to a wide range of bulk gases (usually N_2, O_2, H_2, He and Ar). Fourier Transform Infrared spectroscopy (FTIR) is a well-established technique in the field, enabling detection of multiple species, including water vapor. However, the use of more selective and powerful near-infrared laser-based techniques, such as Tunable Diode Laser Spectroscopy (TDLAS) [12–15] and Cavity Ring-Down Spectroscopy (CRDS) [16–24], has increased significantly within the last decades, leading to the development (and commercialization in some cases) of several dedicated moisture analyzers. The interest in CRDS has enormously increased due to the possibility of using continuous wave (cw) diode laser sources, which are small, can operate at ambient temperature, and can guarantee high repetition rates. In particular, cw-CRDS instruments have proven to be robust [25], suitable for in situ applications [16], having a high dynamic range spanning the reported detection limit from few ppb to hundreds of part-per-trillion (ppt) [18,25]. Moreover, scientists at the National Metrology Institute of Japan successfully tested the performances of cw-CRDS moisture analyzer in terms of achievable accuracy traceable to the International System of Units (SI). In fact, by means of a direct comparison with their primary trace-moisture national standard, water concentrations in nitrogen gases were measured with an overall standard uncertainty of approximately 4% down to approximately mole fraction level of 10 ppb [17]. A similar work has been also performed at the National Institute of Standard and Technologies (USA) in 2009. In particular, by means of an experimental setup which incorporated frequency-stabilized cavity ring-down spectroscopy and a primary standard humidity generator, scientists at NIST could provide very refined determinations of the spectroscopic parameters of fifteen water vapor rovibrational transitions, with an overall combined uncertainty for line intensities below the 0.4% level [26].

More recently, cw-CRDS has also benefitted from the use of near-infrared optical frequency combs synthesizer (OFCS). Because of their fine, discrete and stable spectral structure, OFCSs represent the ideal tool to be combined with cw-CRDS to achieve high precision and accuracy, along with high sensitivity. In this context, many experiments have been performed on water vapor, demonstrating that the combined use of cw-CRDS and OFCS allows for high-quality spectral acquisitions even at trace H_2O amounts [27,28]. Moreover, as far as trace water measurements are concerned, the development of OFCS assisted cw-CRDS experiments enabled for absolute determinations of the molecular number density (that can be easily converted in water mole fraction if the pressure and the temperature of the gas under test are known), while preserving the highest levels of sensitivity [19,20].

In this work, we report on the results of trace water measurements performed by means of a comb-assisted continuous wave cavity ring-down spectrometer (CA-CRDS). Working at the wavelength of 1.39 μm, where high-reflectivity mirrors, high-quality optical components, as well as high-responsivity detectors are available, we were able to measure trace level water content in high-purity N_2 gases. Selecting the most suitable water transition accessible in operation range of our lasers, namely with the spectrometer operating at 7170.27781 cm^{-1} in coincidence with the $3_{2,2}\rightarrow2_{2,1}$ H_2O transition of the $\nu_1+\nu_3$ combination band, we demonstrated the measurement of water vapor amount fractions down to about 380 ppb, with a statistical uncertainty of 5 ppb, for an integration time of 0.2 s. Furthermore, we show that, in its present configuration, the spectrometer can afford a detection limit as low as 160 part per trillion (ppt) by increasing the integration time up to 6 s.

2. Experimental setup

A diagram of the comb-assisted cavity ring-down spectrometer is depicted in Fig. 1. This apparatus represents an upgraded version of the setup already described in Ref. [19]. This second-generation setup has been specifically developed with the aim of further lowering the ultimate sensitivity, the main elements of novelty being a new set of mirrors having a higher reflectivity, a Booster Optical Amplifier (BOA) used to increase the available optical power, and a more efficient system for switching off the laser light.

The core of the experimental setup consists of two phase-locked external cavity diode lasers (ECDL). One of them, the probe laser (PL), is forced to maintain a precise frequency offset from a reference laser (RL), which, in turn, is referenced to an optical frequency comb synthesizer (OFCS). The probe laser emits near-infrared radiation at approximately 1.4 μm and is phase-locked to the RL. At this purpose, a beat note signal between the two lasers is detected by means of a 12-GHz bandwidth photodiode and used to tightly lock the PL to the RL with a variable frequency offset, f_{OFF}. This latter is controlled using a radio frequency synthesizer (RFS) in order to perform frequency scans of the PL across a particular frequency. On the other hand, the reference laser is locked to a high finesse cavity using the Pound–Drever–Hall (PDH) technique, so as to narrow its emission linewidth down to 10 kHz (at 1-ms of observation time). In turn, the PDH cavity is stabilized against one of the optical teeth of the OFCS with an offset frequency of f_{BEAT} = 20 MHz. The OFCS is a self-referenced fiber-based device locked to the 10-MHz time base signal provided by a GPS-disciplined Rb-clock. The relative stability of the RL frequency with respect to the OFCS is 2×10^{-14} at 1 s [29].

The interrogation of the gas samples, by means of the PL, takes place into a high-finesse ring-down (HFRD) cavity. This latter is composed of two plano-concave mirrors with a radius of curvature of 1 meter, having a nominal reflectivity exceeding 99.99%. The mirrors are mounted on a Zerodur® spacer at a distance of 43 cm. One of the mirrors is equipped with a piezoelectric transducer (PZT) to enable a fine-tuning of the cavity length. A 100-Torr absolute pressure gauge (MKS Baratron, mod. AA0612TRA) and a calibrated 100 Ω pt-resistance thermometer allow for the accurate reading of the gas pressure and cavity temperature, respectively. Both the instruments have an accuracy of 0.05%. Two stainless steel vacuum feed-throughs, glued on the Zerodur® spacer, are used in conjunction with a scroll pump to establish high vacuum conditions or to maintain a constant gas flow into the cavity.

Before being coupled into the cavity, the PL beam passes through a free space acousto-optic modulator (AOM) driven at a frequency of f_{AOM} = 80 MHz and is then amplified up to approximately 20 mW by the BOA. Both the AOM and BOA act as optical switches to instantaneously turn off the probe laser and initiate the ring-down decays. As described in Ref. [30], the combined use of the BOA and AOM makes it possible to reach a higher extinction efficiency of the cavity-coupled light and, thereby, ensures a higher signal-to-noise ratio for the recorded ring-down events [31]. At the input of the cavity, the frequency of the PL turns out to be $f_{PL} = N \times f_{REP} + f_{CEO} + f_{BEAT} + f_{OFF} + f_{AOM}$, where N is the comb tooth order, f_{REP} = 250 MHz and

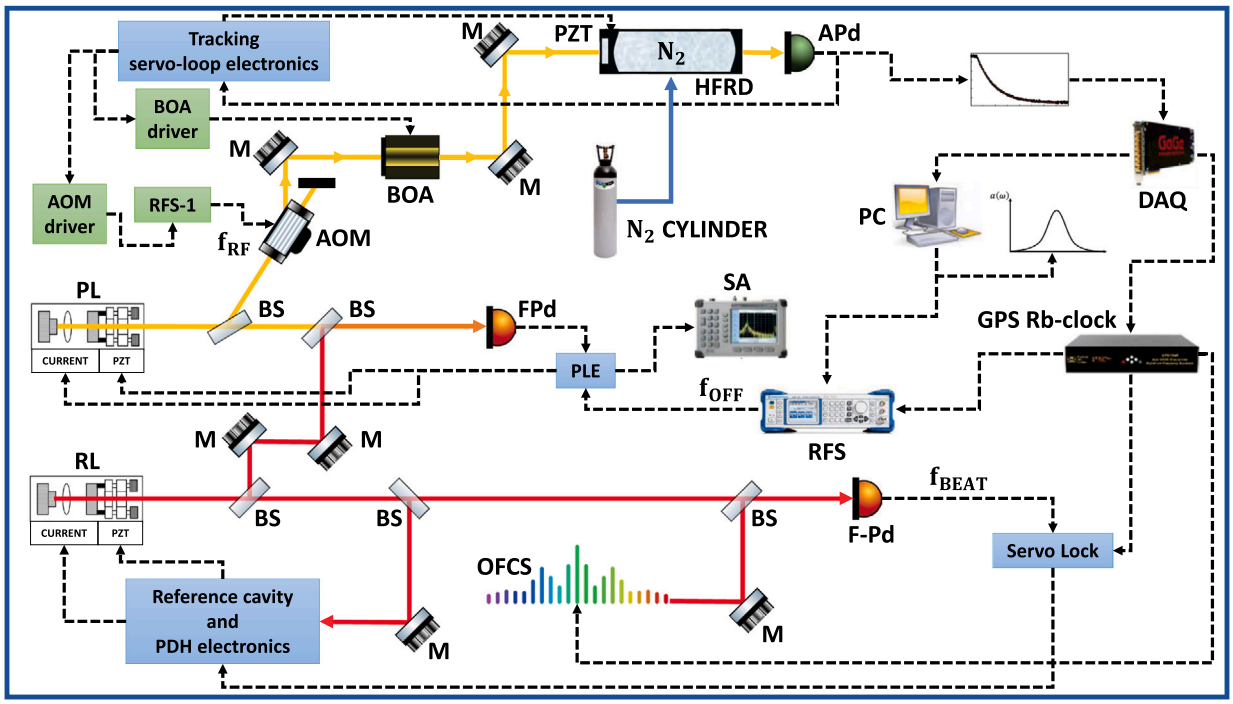

Fig. 1. Schematic diagram of the CA-CRDS. OFCS stands for optical frequency comb synthesizer; RL, reference laser; PL, probe laser; BS, beam splitter; M, mirror; HFRD, high-finesse ring-down cavity; FPd, fast photodiode; AOM, acoustic-optic modulator; BOA, booster optical amplifier; APd, avalanche photodetector; PC, personal computer; RFS, radio-frequency synthesizer; RFS-1, radio-frequency switches; PZT, piezoelectric transducer; DAQ, data acquisition board; PLE, phase-locking electronics, SA, spectrum analyzer. The dashed lines represent electrical connections, while red or yellow lines the path of the laser radiation. (For interpretation of the references to color in this figure legend, the reader is referred to the web version of this article.)

f_{CEO} = 20 MHz are the OFCS repetition rate and carrier-envelope offset frequency, respectively.

The light emerging from the HFRD cavity is monitored by an InGaAs avalanche photodetector (APd). At a fixed frequency of the PL, a tracking servo-loop circuit moves the PZT until a resonance occurs. Once the signal reaches a predetermined threshold level, a TTL signal is sent to the AOM and to the BOA to abruptly switch off the laser light. This triggers a ring down event, which is recorded using a 16-bit resolution digitizer board with a sample rate of 10 MS/s. Before changing the PL frequency, multiple ring-down events can be recorded, each of them being acquired with 1400 points while the light is kept turned off for about 700 μs. The acquisition board and the RFS are referred to the Rb clock and controlled by a computer by means of a Labview code.

3. Results and discussion

To assess the reproducibility of the CA-CRDS we acquired several consecutive ring-down events at a fixed PL frequency under vacuum conditions and we performed an Allan-Werle deviation analysis of these data. In panel (a) of Fig. 2, 50 500 consecutive decay times, recorded in about thirty-five minutes, are displayed. On panel (b) their distribution is plotted, along with a Gaussian fit. The mean value for the ring down times and the standard deviation obtained are τ_0 = 127.5 μs and σ_{τ_0} = 0.05 μs, respectively, leading to a relative standard uncertainty of 0.04%. Similar results have been achieved at different PL frequencies, showing a considerably high reproducibility on a day-by-day basis. The ring-down time of the empty cavity yields a cavity finesse value of 279 000, which corresponds to a cavity mode width of $\Delta\nu_c$ = 1.2 kHz and an effective optical path of about 76 km. From the Allan-Werle deviation behavior (see panel (c) of Fig. 2), σ_A, as function of the integration time, t, the sensitivity of the CA-CRDS can be inferred in terms of the minimum detectable absorption coefficient $\alpha_{min} = \frac{\sigma_A}{c\tau_0^2}$ or in terms of noise equivalent absorption coefficient $NEA = \frac{\sigma_{\tau_0}}{c\tau_0^2}\sqrt{\frac{2}{f_{RATE}}}$, f_{RATE} = 23 Hz being the repetition rate of the ring down acquisitions. The Allan-Werle deviation decrease as $t^{-1/2}$, as expected for a white noise distribution, down to a minimum value of $\sigma_{A_{min}} = 3.1 \times 10^{-3}$ μs, for an optimum integration time of about 6 s, corresponding to a number of the ring-down events equals to N = 138. The α_{min} and NEA, retrieved turn out to be 6.5×10^{-12} cm^{-1} and 3.1×10^{-11} $\frac{\text{cm}^{-1}}{\sqrt{\text{Hz}}}$, respectively.

Fig. 3, panel (a), shows a typical absorption spectrum of the H_2O $3_{2,2}\rightarrow 2_{2,1}$ transition, belonging to $\nu_1 + \nu_3$ vibrational band, acquired under a continuous flow of high purity N_2 gas, keeping a constant pressure value in the cavity of 2133 Pa. The PL laser frequency scan around the line center was about 4.8 GHz, consisting a spectrum of 60 uniformly spaced spectral points. Each point is the average of five consecutive ring-down events, the time necessary to record the full spectrum being 15 s. The absorption coefficient, $\alpha(\nu)$, was retrieved from the ring down time, τ (in s), as function of the PL frequency ν (in cm^{-1}) following the well-known equation $\alpha(\nu) = \frac{1}{c}\left(\frac{1}{\tau} - \frac{1}{\tau_0}\right)$, being τ_0 the ring down time under vacuum conditions. To evaluate the water mole fraction we used the expression:

$$X_W = \frac{\alpha_{TOT} k_B T}{S(T) p} \tag{1}$$

where k_B is the Boltzmann constant, T is the thermodynamic temperature, p is the gas pressure, and $S(T)$ is the line intensity. The integrated absorption coefficient, given by $\alpha_{TOT} = \int \alpha(\nu) d\nu$, was determined by means of a nonlinear least-squares fit of the absorption spectrum using the following equation:

$$\alpha(\nu) = (P_0 + P_1\nu) + \alpha_{TOT} g(\nu - \nu_0). \tag{2}$$

Here, the linear baseline takes into account a residual frequency-dependence of mirrors' reflectivity, while $g(\nu - \nu_0)$ represents a normalized line shape profile having its center at ν_0.

In order to determine the most suitable line shape model, we conducted a comparative analysis of five different profiles. The optimal

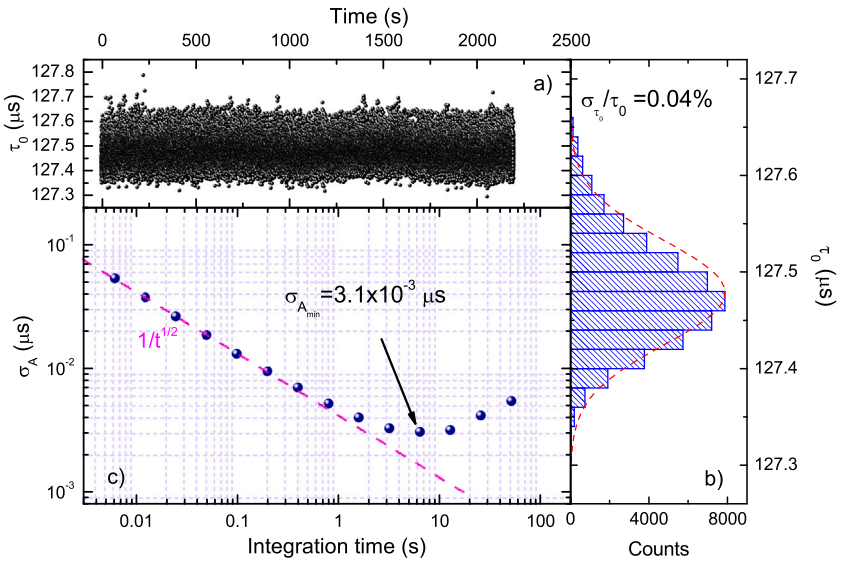

Fig. 2. Panel (a): 50 500 decay times acquired at fixed PL frequency. Panel (b): Statistical distribution of data in (a). Panel (c): Allan-Werle deviation analysis of the measured ring down times.

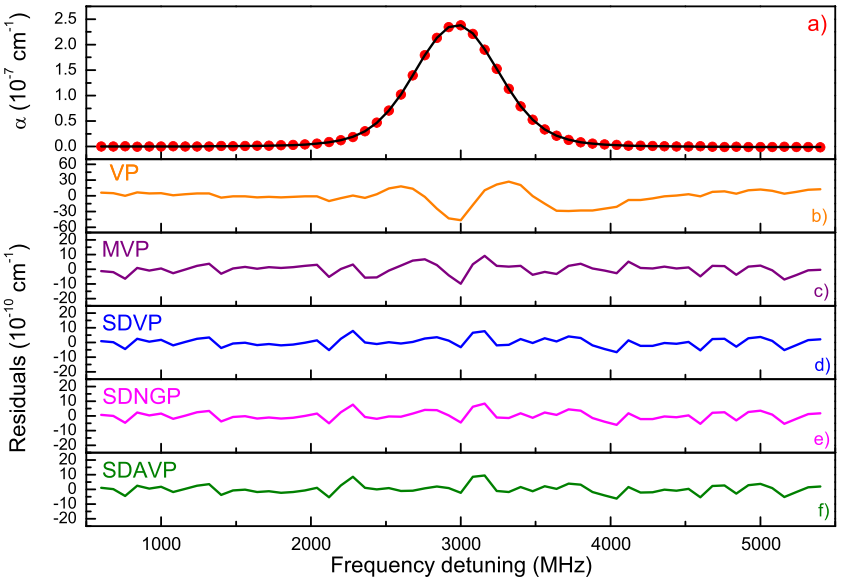

Fig. 3. Panel (a): experimental H_2O absorption spectrum recorded at a total pressure of about 2 kPa of high purity nitrogen gas. Panels (b), (c), (d), e, and (f): residuals resulting from the nonlinear least-squares fit of Eq. (2) by means of a VP, MVP, SDVP, SDNGP, and SDAVP, respectively.

model was selected by comparing the root mean square (rms) of the residuals and applying the so-called Akaike information criterion (AIC) [32], following the same approach adopted in Ref. [33]. The AIC is a statistical estimator that provides information about the risk of overfitting the data by adding parameters in a model. The quantity q_{AIC} is defined according to the following equation:

$$q_{AIC} = N_p[\ln\{\sigma_f\}^2 + \ln(2\pi) + 1] + 2(P_{fit} + 1), \quad (3)$$

where P_{fit} is the number of the parameters used in the fitting procedure, N_p the number of the spectral points, and $\{\sigma_f\}$ the numerical value of the residuals' rms. This quantity makes it possible to evaluate if an increased number of parameters brings to a real improvement of the fit's quality or leads to a penalty related to an useless complexity of the model. If two different models lead to similar rms values, the q_{AIC} parameter can be used to infer which model is the optimal one. In particular, a lower q_{AIC} value for a model means less risk of overfitting, namely a better model.

Several alternatives to the well-known Voigt profile (VP), with increasing complexity, have been proposed for the analysis of water absorption spectra [26,34,35]. A detailed review is out of the aim of this paper and we refer the reader to Ref. [36] for a more detailed description. Here, $g(\nu - \nu_0)$ was modeled using the VP, the modified Voigt Profile (MVP), the speed-dependent Voigt profile (SDVP), the speed-dependent Nelkin–Ghatak profile (SDNGP), and the speed-dependent asymmetric Voigt profile (SDAVP). We draw the attention of the readers on the fact that a MVP is a VP in which the Doppler width is left as a free parameter during the spectra analysis. In the case of speed-dependent profiles, the speed dependence of collisional broadening and shifting is considered in a quadratic form [37]. With the exception of the MVP, for all the investigated line shape models the Doppler width (Γ_D) of the line was fixed to the value calculated from the measured temperature. The collisional width (Γ_L) was left as free parameter for all the profiles, while a parameter describing the speed-dependence of the collisional broadening (a_w) was included for the SDVP, the SDNGP, and the SDAVP. Following the outcomes of Ref. [26], the collisional

Table 1
P_{fit}, q_{AIC}, QF, and the rms values for the all the investigated line shape functions.

$g(\nu-\nu_0)$	rms (cm^{-1})	QF	P_{fit}	q_{AIC}
VP	1.69×10^{-9}	141	5	−2241.5
MVP	3.33×10^{-10}	715	6	−2434.5
SDVP	2.84×10^{-10}	838	6	−2453.6
SDNGP	2.80×10^{-10}	850	7	−2453.3
SDAVP	2.75×10^{-10}	866	8	−2453.4

shifting coefficient, δ, was constrained to the value reported in the HITRAN database for the air-induced shifting [38]. When both the Dicke narrowing and the speed-dependence were taken into account, namely when the SDNGP was used, a collisional narrowing parameter (β) was also considered. Instead, in the case of the SDAVP, a parameter describing the speed-dependence of the collisional shifting (a_s) was included. Finally, for all the models, the baseline coefficients, P_0 and P_1, the unperturbed line center frequency ν_0, and α_{TOT} were considered as variable quantities.

The fit residuals, as obtained from a Levenberg–Marquardt χ^2 minimization routine, are reported in Fig. 3, while in Table 1 we summarized the P_{fit}, the q_{AIC}, the quality of fit parameter, QF, and the rms values corresponding to all the investigated line shape models. It is useful to remind that the QF parameter is defined as the ratio of the peak absorption to the standard deviation of the fit residuals.

As expected, the Voigt model is incapable of fitting the measured spectrum at the present noise level and yields an overly broad profile, as evinced by the clear asymmetric "w" structure in the residuals of panel b. This result is consistent with the omission of any line narrowing mechanism. As confirmation of fact that this mechanism has to be properly taken into account, we can highlight that when Γ_D was left as free, namely when the MVP was adopted, the quality of the fit was poorly improved, being the "w" structure still visible (see panel c). Indeed, when the speed-dependence and the Dicke narrowing are considered, the magnitude of the residuals reduced. On the other hand, the calculated q_{AIC} values revealed that all the speed dependent models were almost equivalent. However, the SDAVP seems to be the most appropriate choice that guarantees the lowest rms value. It is worth noting that this result is in full agreement with the conclusions of the work performed by Hashigushi et al. [33].

In order to quantify the sensitivity of the CA-CRDS spectrometer, in terms of minimum detectable water mole fraction, $X_{W_{min}}$, the following expression can be used [39]:

$$X_{W_{min}} = \frac{\alpha_{rms} k_B T}{p S g_{SDAVP}(0)}. \quad (4)$$

In this expression, α_{rms} represents the rms of the fit residuals and $g_{SDAVP}(0)$ is the value of the SDAVP at the line center frequency. In the experimental conditions of Fig. 3, an $X_{W_{min}}$ value of 7 ppb can be derived. The limit of detection (LOD), which depends on the integration time of each spectral point of the acquired spectra, can be furtherly improved. In particular, averaging over 138 ring down events, namely for an integration time of 6 s (corresponding to the minimum of the Allan-Werle plot of Fig. 2), the minimum absorption coefficient decreases by more than one order of magnitude down to 6.36×10^{-12} cm^{-1}. As a result, a LOD of 160 ppt can be estimated. It is worth noting that this result represents an improvement of about one order of magnitude as compared to what we achieved by means of our first generation spectrometer [19]. The upgrades to the spectrometer, namely, the use of better mirrors, the BOA, and the more efficient light switching-off system, contributed almost equally to the reduction of the minimum detectable absorption coefficient.

Fig. 4 displays an example of continuous monitoring of the water mole fraction in a gas stream of pure nitrogen from a gas cylinder having a nominal residual moisture content of less than 500 ppb. The measurements were performed with the gas flowing through the HFRD cavity at about 2 l/min, while the pressure was kept to a constant value of 2666 Pa by means of a pressure-forward controller (Bronkhorst, mod. 602C-AAA-00A1). In addition, we must highlight that for the retrieving of the data of Fig. 4, each absorption spectrum was acquired with a horizontal resolution of 120 spectral points, while the frequency span was the same as that of Fig. 3.

Although both the HFRD Zerodur® cavity and the stainless steel fittings with the gas cylinder were maintained under vacuum conditions, with the turbomolecular pump turned on for several days before starting the measurements campaign, and the spectra acquisition was performed under continuous gas flow conditions, a clear evidence of a strong memory effect was observed. Indeed, water can be adsorbed and desorbed while the moist nitrogen is flowing through the tubing and the cavity spacer, thus resulting in a change of the measured gas concentrations. Molecules with a large and permanent dipole moment, such as water, have a strong tendency to stick to surfaces. The adsorption/desorption processes depend both on the experimental conditions (the gas flow, in particular), and on physical properties of the internal surface (material, temperature, porosity). The internal wall surfaces of the tubes and cavity can be considered as a place with free binding sites for H_2O as well as a reservoir of absorbing molecules. Thereby, in principle, adsorption/desorption processes need to be properly taken into account if an accurate determination of the water content has to be performed. While the N_2 is flowing in the gas line, a dynamic equilibrium condition needs to be achieved between the so-called surface coverage and molecules concentration. Therefore, flowing the gas through the cavity, a satisfactory determination of the water concentration could be performed only when a steady-state condition is reached.

The equilibrium between adsorption/desorption processes could be theoretically investigated and modeled [40,41]. This would involve the solution of a rather complicated partial differential equation in which the time and spatial derivatives of the H_2O concentration, the surface coverage, the velocity of the gas flow, and the particular geometry of experimental setup would be properly considered to derive a sort of mass conservation law. This is a quite ambitious task for our CA-CRDS spectrometer, especially in reason of the presence of materials with different porosity. On the other hand, a solution to this problem would be out of the aim of this work. Nevertheless, we expect that the time evolution of the measured water concentration may show a multi-exponential behavior in which the different decay rates are determined by the adsorption/desorption processes from the different materials as well as by the geometry of the setup [41].

For the experimental data of panel (a) of Fig. 4, the following expression has been used to model the time evolution of X_W:

$$X_W = X_{W_\infty} + A_1 \exp\left(-\frac{t}{\tau_1}\right) + A_2 \exp\left(-\frac{t}{\tau_2}\right) + A_3 \exp\left(-\frac{t}{\tau_3}\right), \quad (5)$$

where X_{W_∞} represents the water mole fraction when the steady-state condition is reached, A_i and τ_i, are the amplitude and the decay time constant of each exponential term, respectively. We note the excellent agreement between the experimental and theoretical values, as clearly evidenced by the fit residuals reported in panel (b) of Fig. 4, whose rms value amounts to 7 ppb. If a double exponential law is used, the residuals' rms-value increases up to 26 ppb, due to the clear structure that is shown in panel (c) of Fig. 4. The decay time constants, as retrieved from the fit to Eq. (5), are $\tau_1 = 684 \pm 13$ s, $\tau_2 = 4319 \pm 117$ s, and $\tau_3 = 147 \pm 3$ s.

As far as the fit of Fig. 4 is concerned, it is worth noting that the change in the reduced χ^2 that results from the addition of a fourth exponential term in Eq. (5) is not statistically significant, as clearly indicated by an F-test performed with a confidence level of 5%. Moreover, the application of the Akaike information criterion confirms that a four-exponential model increases the risk of overfitting. However, if we consider the possibility that a fourth exponential decay could be hidden by the limited acquisition time, a fitting function that takes into account

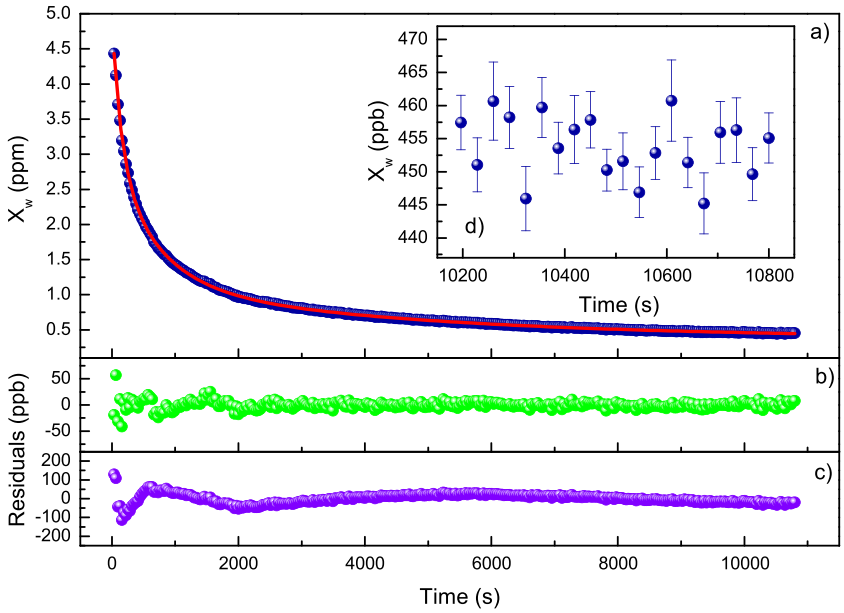

Fig. 4. Panel (a): Time development of the CA-CRDS measured water mole fraction. The N_2 flow rate in the HFRD cavity was 2 l/min while the gas pressure was set to the constant value of 2666 Pa. The dispersion of the points, for each determination, is not visible, being much smaller than the size of the points. Panel (b): residuals resulting from the fit of the data of panel (a) to the sum of three exponential decay functions as given by Eq. (5). Panel (c): the same as panel (b) with two exponential decays. Panel (d): last twenty experimental points of the data depicted in panel (a).

a further adsorption/desorption process leads to the determination of an asymptotic mole fraction value that fully agrees with the retrieved X_{W_∞} value of 382 ppb, within its statistical uncertainty.

It must be noted that the inner surface of the Zerodur® spacer (~300 cm^2) is roughly a factor of 2 larger than that of the 1-m long electro-polished stainless tube (with a 6.35-mm outer diameter) used to connect the gas cylinder to the HFRD cavity. Moreover, the porosity of the stainless steel is surely much smaller than that of the Zerodur® spacer, due to the different quality of the polishing treatments. Therefore, the longest decay time is most likely attributable to the Zerodur® spacer. According to our experimental findings, we can conclude that, before a steady-state condition is reached, a considerable long time span (more than four hours) is needed, a circumstance that represents the main limiting factor of the present spectrometer. On the other hand, we can state that the X_{W_∞} value of 382 ± 5 ppb, as retrieved from the multi-exponential fit, can provide a satisfactory estimate of the residual water content in the gas cylinder. It must be noted that the value of the asymptotic water mole fraction is rather different from the one resulting from the tail of the experimental curve of Fig. 4. In particular, if we look at the last 600 s of continuous measurements, namely at the last twenty X_W determinations (see the inset of Fig. 4), the average value of the water mole fraction results to be 454 ± 5 ppb. This discrepancy is not surprising if we consider that the transient behavior described above covers a time span that exceeds our measurement time.

In an effort to estimate the combined relative uncertainty associated with the X_W measurements, the possible sources of uncertainty have been identified and classified as Type A and Type B. These contributions, corresponding to one standard deviation ($k = 1$), are summarized in relative terms in Table 2. The Type A uncertainty, which amounts to the 1.3%, can be assumed to be the statistical uncertainty on X_{W_∞} as retrieved from the multi-exponential fit. The principal sources of Type B uncertainty are those related to (i) the line strength, (ii) the frequency scale, (iii) the amplitude of the laser scan, (iv) the choice of the line shape model adopted in Eq. (2), (v) the partition function, (vi) the number of spectral point, (vii) the integration time of each spectral point, (viii) the temperature, and (ix) the pressure of the gas. With respect to the line strength of the $3_{2,2}\rightarrow2_{2,1}$ H_2O transition, we must consider that the value used in Eq. (1), namely $S = 2.0158 \times 10^{-21}$ cm/molecule, was the one provided by Lisak et al. in Ref. [26] having

Table 2
Uncertainty budget related to the spectroscopic determination of the water mole fraction. Each contribution represents the 1-σ uncertainty in relative term.

Contribution ($k = 1$)	Type A (%)	Type B (%)
Statistical	1.3	
Line strength		0.3
Frequency scale		Negligible
Laser scan width		0.08
Line shape model		0.1
Horizontal resolution of the frequency scale		0.2
Integration time of each spectral points		Negligible
Partition function		0.04
Temperature		0.07
Pressure		0.05
Overall combined uncertainty (%)	1.4	

an overall uncertainty of 0.3%. As far as the linearity of the frequency scale is concerned, according to Ref. [29], we can infer as negligible this contribution. Another component of uncertainty that could influence the accuracy of the frequency scale is related to the frequency difference between the probe (excitation) laser and the cavity resonance, as clearly explained by Reed et al. [42]. In our experimental conditions, the maximum deviation between the two frequencies amounts to about 1 kHz, for each transient cavity build-up event. Due to the five repeated acquisitions of the cavity decay time for each spectral point, such a deviation should be divided by $5^{1/2}$, thus leading to a Type-B contribution of ~447 Hz, which makes this contribution completely negligible. In order to evaluate the uncertainty due to the laser scan width, we performed several determinations of X_W as function of the width of the frequency interval underneath the experimental spectra. If the frequency span is reduced, so as to approach the full-width at half-maximum (FWHM) of the absorption line, a systematic error in the determination of α_{TOT} is introduced, which, in turn, influences X_W. In the case of the spectrum of Fig. 2, in which the frequency scan is more than six times wider than the FWHM, we estimated this contribution to be at the level of 0.08%. Regarding the possible impact of the choice of line shape function on the integrated absorption coefficient determinations, we solely compared the results obtained by using of the SDVP, SDNGP, and SDAVP, being the inadequacy of the

VP in reproducing the experimental spectra clearly evident from the residuals of panel (b) of Fig. 3. The determination of the mole fraction appeared to be quite robust regardless of the choice of the particular line shape model. The upper limit for this source of uncertainty was estimated to be 0.1%. Several measurement campaigns have shown that the integration time of each spectral point had a negligible influence on the retrieved X_W value, while the horizontal resolution of the frequency scale needs to be taken into account with a 0.2% entry in Table 2. A further source of Type B uncertainty could be ascribed to the partition function. Since $Q(T)$ comes into play during the rescaling of S to the actual temperature of the gas, its uncertainty must be properly taken into account. Following the outcomes of [43,44], we found that this additional contribution amounts to 0.04%. Finally, the effects of temperature and pressure uncertainties are found to be 0.07 and 0.05%, respectively. By adding in quadrature all the contributions, the combined relative standard uncertainty was estimated to be 1.4% for a water concentration range from a few ppm down to about 300 ppb.

4. Conclusions

In summary, we demonstrated continuous sub-ppm measurements of water mole fractions in a ultra-high purity nitrogen gas with a relative uncertainty of 1.4%, by means of a second-generation comb-assisted cavity ring-down spectrometer. The complete uncertainty budget is performed after quantifying all the possible sources of systematic uncertainties. The ultimate sensitivity of the set-up was carefully determined by using an Allan-Werle deviation analysis, thus leading to a H_2O limit of detection of 160 part per trillion, for an integration time of 6 s. This latter corresponds to a H_2O partial pressure of 3.4×10^{-7} Pa. Improvements that will be implemented in the near future include the replacement of the Zerodur® cavity spacer with a new one made of 316L-type stainless steel with an electropolished inner surface, properly treated with a hydrophobic coating. This is expected to significantly reduce water adsorption and desorption phenomena, minimizing the transient to a steady-state condition and thus reducing the total acquisition time. In addition, the spectrometer will be constructed in a more compact way using integrated, fiber coupled, optical devices, thus reducing the optical path length in air as much as possible.

CRediT authorship contribution statement

Eugenio Fasci: Investigation, Writing – original draft. **Muhammad Asad Khan:** Investigation, Data curation. **Vittorio D'Agostino:** Investigation, Data curation. **Stefania Gravina:** Investigation, Data curation. **Vito Fernicola:** Writing – review & editing, Funding acquisition. **Livio Gianfrani:** Conceptualization, Writing – review & editing, Supervision, Funding acquisition. **Antonio Castrillo:** Conceptualization, Data analysis, Writing – review & editing.

Declaration of competing interest

The authors declare that they have no known competing financial interests or personal relationships that could have appeared to influence the work reported in this paper.

Data availability

Data will be made available on request.

Acknowledgment

The authors thank G. Porzio for his technical support.

Funding

This work was done within the project PROMETH2O (EMPIR 20IND06), which received funding from the EMPIR programme co-financed by the Participating States and from the European Union's Horizon 2020 research and innovation programme.

References

[1] R.X. Adhikari, K. Arai, A.F. Brooks, C. Wipf, O. Aguiar, P. Altin, B. Barr, L. Barsotti, R. Bassiri, A. Bell, G. Billingsley, R. Birney, D. Blair, E. Bonilla, J. Briggs, D.D. Brown, R. Byer, H. Cao, M. Constancio, S. Cooper, T. Corbitt, D. Coyne, A. Cumming, E. Daw, R. deRosa, G. Eddolls, J. Eichholz, M. Evans, M. Fejer, E.C. Ferreira, A. Freise, V.V. Frolov, S. Gras, A. Green, H. Grote, E. Gustafson, E.D. Hall, G. Hammond, J. Harms, G. Harry, K. Haughian, D. Heinert, M. Heintze, F. Hellman, J. Hennig, M. Hennig, S. Hild, J. Hough, W. Johnson, B. Kamai, D. Kapasi, K. Komori, D. Koptsov, M. Korobko, W.Z. Korth, K. Kuns, B. Lantz, S. Leavey, F. Magana-Sandoval, G. Mansell, A. Markosyan, A. Markowitz, I. Martin, R. Martin, D. Martynov, D.E. McClelland, G. McGhee, T. McRae, J. Mills, V. Mitrofanov, M. Molina-Ruiz, C. Mow-Lowry, J. Munch, P. Murray, S. Ng, M.A. Okada, D.J. Ottaway, L. Prokhorov, V. Quetschke, S. Reid, D. Reitze, J. Richardson, R. Robie, I. Romero-Shaw, R. Route, S. Rowan, R. Schnabel, M. Schneewind, F. Seifert, D. Shaddock, B. Shapiro, D. Shoemaker, A.S. Silva, B. Slagmolen, J. Smith, N. Smith, J. Steinlechner, K. Strain, D. Taira, S. Tait, D. Tanner, Z. Tornasi, C. Torrie, M.V. Veggel, J. Vanheijningen, P. Veitch, A. Wade, G. Wallace, R. Ward, R. Weiss, P. Wessels, B. Willke, H. Yamamoto, M.J. Yap, C. Zhao, A cryogenic silicon interferometer for gravitational-wave detection, Classical Quantum Gravity 37 (16) (2020) 165003, http://dx.doi.org/10.1088/1361-6382/ab9143.

[2] H.H. Funke, B.L. Grissom, C.E. McGrew, M.W. Raynor, Techniques for the measurement of trace moisture in high-purity electronic specialty gases, Rev. Sci. Instrum. 74 (9) (2003) 3909–3933, http://dx.doi.org/10.1063/1.1597939.

[3] ITRS, The international technology roadmap for semiconductors, 2011, http://www.itrs2.net/2013-itrs.html.

[4] T. Watanabe, H.H. Funke, R. Torres, M.W. Raynor, J. Vininski, V.H. Houlding, Contamination control in gas delivery systems for MOCVD, J. Cryst. Growth 248 (2003) 67–71, http://dx.doi.org/10.1016/S0022-0248(02)01889-4.

[5] K. Siefering, H. Berger, W. Whitlock, Quantitative analysis of contaminants in ultrapure gases at the parts-per-trillion level using atmospheric pressure ionization mass spectroscopy, J. Vac. Sci. Technol. A 11 (4) (1993) 1593–1597, http://dx.doi.org/10.1116/1.578510.

[6] E. Flaherty, C. Herold, D. Murray, S.R. Thompson, Determination of water in hydrogen chloride gas by a condensation technique, Anal. Chem. 58 (8) (1986) 1903–1904, http://dx.doi.org/10.1021/ac00121a070.

[7] V. Manickam, E. Prabhu, V. Jayaraman, K. Gnanasekar, T. Gnanasekaran, K. Nagaraja, Electrolytic sensor for trace level determination of moisture in gas streams, Measurement 43 (10) (2010) 1636–1643, http://dx.doi.org/10.1016/j.measurement.2010.09.023.

[8] C. O'Sullivan, G. Guilbault, Commercial quartz crystal microbalances – theory and applications, Biosens. Bioelectron. 14 (8) (1999) 663–670, http://dx.doi.org/10.1016/S0956-5663(99)00040-8.

[9] R.K. Nahar, Physical understanding of moisture induced degradation of nanoporous aluminum oxide thin films, J. Vac. Sci. Technol. B: Microelectron. Nanometer Struct. Process. Meas. Phenom. 20 (1) (2002) 382–385, http://dx.doi.org/10.1116/1.1430243.

[10] A.I. Buvailo, Y. Xing, J. Hines, N. Dollahon, E. Borguet, TiO_2/LiCl-based nanostructured thin film for humidity sensor applications, ACS Appl. Mater. Interfaces 3 (2) (2011) 528–533, http://dx.doi.org/10.1021/am1011035, pMID: 21284374.

[11] T. Jifang, L. Yu, W. Li, C. Hong, S. Tao, S. Junfeng, L. Hui, G. Yuandong, An ultrahigh-accuracy miniature dew point sensor based on an integrated photonics platform, Sci. Rep. 6 (2015) 29672, http://dx.doi.org/10.1038/srep29672.

[12] R.S. Inman, J.J.F. McAndrew, Application of tunable diode laser absorption spectroscopy to trace moisture measurements in gases, Anal. Chem. 66 (15) (1994) 2471–2479, http://dx.doi.org/10.1021/ac00087a011.

[13] D.C. Hovde, J.T. Hodges, G.E. Scace, J.A. Silver, Wavelength-modulation laser hygrometer for ultrasensitive detection of water vapor in semiconductor gases, Appl. Opt. 40 (6) (2001) 829–839, http://dx.doi.org/10.1364/AO.40.000829.

[14] S. Pal, A. Das, S. Nandy, R. Kar, J. Ghosh, Development of a near-infrared tunable diode laser absorption spectrometer for trace moisture measurements in helium gas, Rev. Sci. Instrum. 90 (10) (2019) 103105, http://dx.doi.org/10.1063/1.5113968.

[15] W. Nie, Z. Xu, R. Kan, J. Ruan, L. Yao, B. Wang, Y. He, Development of a dew/frost point temperature sensor based on tunable diode laser absorption spectroscopy and its application in a cryogenic wind tunnel, Sensors 18 (8) (2018) http://dx.doi.org/10.3390/s18082704.

[16] H. Abe, K. Hashiguchi, D. Lisak, S. Honda, T. Miyake, H. Shimizu, A miniaturized trace-moisture sensor based on cavity ring-down spectroscopy, Sensors Actuators A 320 (2021) 112559, http://dx.doi.org/10.1016/j.sna.2021.112559.

[17] H. Abe, K.M. Yamada, Performance evaluation of a trace-moisture analyzer based on cavity ring-down spectroscopy: Direct comparison with the NMIJ trace-moisture standard, Sensors Actuators A 165 (2) (2011) 230–238, http://dx.doi.org/10.1016/j.sna.2010.11.005.

[18] K. Hashiguchi, D. Lisak, A. Cygan, R. Ciuryło, H. Abe, Parts-per-trillion sensitivity for trace-moisture detection using wavelength-meter-controlled cavity ring-down spectroscopy, AIP Adv. 9 (12) (2019) http://dx.doi.org/10.1063/1.5127786.

[19] E. Fasci, H. Dinesan, L. Moretti, A. Merlone, A. Castrillo, L. Gianfrani, Dual-laser frequency-stabilized cavity ring-down spectroscopy for water vapor density measurements, Metrologia 55 (5) (2018) 662, http://dx.doi.org/10.1088/1681-7575/aad15e.

[20] E. Fasci, V. D'Agostino, M.A. Khan, S. Gravina, G. Porzio, L. Gianfrani, A. Castrillo, Comb-assisted cavity ring-down spectroscopy for ultra-sensitive traceable measurements of water vapour in ultra-high purity gases, J. Phys. Conf. Ser. 2439 (1) (2023) 012017, http://dx.doi.org/10.1088/1742-6596/2439/1/012017.

[21] V. Vorsa, S. Dheandhanoo, S.N. Ketkar, J.T. Hodges, Quantitative absorption spectroscopy of residual water vapor in high-purity gases: pressure broadening of the 1.39253-μm H_2O transition by N_2, HCl, HBr, Cl_2, and O_2, Appl. Opt. 44 (4) (2005) 611–619, http://dx.doi.org/10.1364/AO.44.000611.

[22] S.Y. Lehman, K.A. Bertness, J.T. Hodges, Detection of trace water in phosphine with cavity ring-down spectroscopy, J. Cryst. Growth 250 (1) (2003) 262–268, http://dx.doi.org/10.1016/S0022-0248(02)02248-0, proceedings of the Fourteenth American Conference on Crystal Grow th and Epitaxy.

[23] K. Hashiguchi, D. Lisak, A. Cygan, R. Ciuryło, H. Abe, Wavelength-meter controlled cavity ring-down spectroscopy: high-sensitivity detection of trace moisture in N_2 at sub-ppb levels, Sensors Actuators A 241 (2016) 152–160, http://dx.doi.org/10.1016/j.sna.2016.02.016.

[24] H. Abe, M. Amano, K. Hashiguchi, D. Lisak, S. Honda, T. Miyake, Improvement of spectral resolution in a miniaturized trace-moisture sensor using cavity ring-down spectroscopy: Performance evaluation using a trace-moisture standard in he, Sensors Actuators A 351 (2023) 114146, http://dx.doi.org/10.1016/j.sna.2022.114146.

[25] H. Abe, D. Lisak, A. Cygan, R. Ciuryło, Note: reliable, robust measurement system for trace moisture in gas at parts-per-trillion levels using cavity ring-down spectroscopy, Rev. Sci. Instrum. 86 (10) (2015) 106110, http://dx.doi.org/10.1063/1.4934976.

[26] D. Lisak, D.K. Havey, J.T. Hodges, Spectroscopic line parameters of water vapor for rotation-vibration transitions near 7180 cm^{-1}, Phys. Rev. A 79 (2009) 052507, http://dx.doi.org/10.1103/PhysRevA.79.052507.

[27] D. Mondelain, S. Mikhailenko, E. Karlovets, S. Béguier, S. Kassi, A. Campargue, Comb-assisted cavity ring down spectroscopy of^{17}O enriched water between 7443 and 7921 cm^{-1}, J. Quant. Spectrosc. Radiat. Transfer 203 (2017) 206–212, http://dx.doi.org/10.1016/j.jqsrt.2017.03.029, hITRAN2016, Special Issue.

[28] A. Koroleva, S. Mikhailenko, S. Kassi, A. Campargue, Frequency comb-referenced cavity ring-down spectroscopy of natural water between 8041 and 8633 cm^{-1}, J. Quant. Spectrosc. Radiat. Transfer 298 (2023) 108489, http://dx.doi.org/10.1016/j.jqsrt.2023.108489.

[29] A. Castrillo, E. Fasci, H. Dinesan, S. Gravina, L. Moretti, L. Gianfrani, Optical determination of thermodynamic temperatures from a C_2H_2 line-doublet in the near infrared, Phys. Rev. A 11 (2019) 064060, http://dx.doi.org/10.1103/PhysRevApplied.11.064060.

[30] E. Fasci, S. Gravina, G. Porzio, A. Castrillo, L. Gianfrani, Lamb-dip cavity ring-down spectroscopy of acetylene at 1.4μm, New J. Phys. 23 (12) (2021) 123023, http://dx.doi.org/10.1088/1367-2630/ac3b6e.

[31] H. Huang, K.K. Lehmann, Noise caused by a finite extinction ratio of the light modulator in cw cavity ring-down spectroscopy, Appl. Phys. B 94 (2009) 355–366, http://dx.doi.org/10.1007/s00340-008-3293-y.

[32] H. Akaike, Information Theory and an Extension of the Maximum Likelihood Principle, Springer New York, New York, NY, 1998.

[33] K. Hashiguchi, D. Lisak, A. Cygan, R. Ciuryło, H. Abe, Spectral analysis of H_2O near 7180 cm^{-1} to accurately measure trace moisture in N_2 gas: evaluation of line shape profiles using akaike information criterion, Japan. J. Appl. Phys. 61 (1) (2021) 012003, http://dx.doi.org/10.35848/1347-4065/ac3724.

[34] M.D. De Vizia, F. c. Rohart, A. Castrillo, E. Fasci, L. Moretti, L. Gianfrani, Speed-dependent effects in the near-infrared spectrum of self-colliding $H_2^{18}O$ molecules, Phys. Rev. A 83 (2011) 052506, http://dx.doi.org/10.1103/PhysRevA.83.052506.

[35] M.D. De Vizia, A. Castrillo, E. Fasci, P. Amodio, L. Moretti, L. Gianfrani, Experimental test of the quadratic approximation in the partially correlated speed-dependent hard-collision profile, Phys. Rev. A 90 (2014) 022503, http://dx.doi.org/10.1103/PhysRevA.90.022503.

[36] J.-M. Hartmann, C. Boulet, D. Robert, III - Isolated lines, in: J.-M. Hartmann, C. Boulet, D. Robert (Eds.), Collisional Effects on Molecular Spectra, Elsevier, Amsterdam, 2008, pp. 63–145, http://dx.doi.org/10.1016/B978-0-444-52017-3.00003-0.

[37] N. Ngo, D. Lisak, H. Tran, J.-M. Hartmann, An isolated line-shape model to go beyond the voigt profile in spectroscopic databases and radiative transfer codes, J. Quant. Spectrosc. Radiat. Transfer 129 (2013) 89–100, http://dx.doi.org/10.1016/j.jqsrt.2013.05.034.

[38] I. Gordon, L. Rothman, R. Hargreaves, R. Hashemi, E. Karlovets, F. Skinner, E. Conway, C. Hill, R. Kochanov, Y. Tan, P. Wcisło, A. Finenko, K. Nelson, P. Bernath, M. Birk, V. Boudon, A. Campargue, K. Chance, A. Coustenis, B. Drouin, J. Flaud, R. Gamache, J. Hodges, D. Jacquemart, E. Mlawer, A. Nikitin, V. Perevalov, M. Rotger, J. Tennyson, G. Toon, H. Tran, V. Tyuterev, E. Adkins, A. Baker, A. Barbe, E. Canè, A. Császár, A. Dudaryonok, O. Egorov, A. Fleisher, H. Fleurbaey, A. Foltynowicz, T. Furtenbacher, J. Harrison, J. Hartmann, V. Horneman, X. Huang, T. Karman, J. Karns, S. Kassi, I. Kleiner, V. Kofman, F. Kwabia-Tchana, N. Lavrentieva, T. Lee, D. Long, A. Lukashevskaya, O. Lyulin, V. Makhnev, W. Matt, S. Massie, M. Melosso, S. Mikhailenko, D. Mondelain, H. Müller, O. Naumenko, A. Perrin, O. Polyansky, E. Raddaoui, P. Raston, Z. Reed, M. Rey, C. Richard, R. Tóbiás, I. Sadiek, D. Schwenke, E. Starikova, K. Sung, F. Tamassia, S. Tashkun, J. Vander Auwera, I. Vasilenko, A. Vigasin, G. Villanueva, B. Vispoel, G. Wagner, A. Yachmenev, S. Yurchenko, The HITRAN2020 molecular spectroscopic database, J. Quant. Spectrosc. Radiat. Transfer 277 (2022) 107949, http://dx.doi.org/10.1016/j.jqsrt.2021.107949.

[39] B. Chen, P. Kang, J.-y. Li, X.-l. He, A.-w. Liu, S.-m. Hu, Quantitative moisture measurement with a cavity ring-down spectrometer using telecom diode lasers, Chin. J. Chem. Phys. 28 (1) (2015) 6–10, http://dx.doi.org/10.1063/1674-0068/28/cjcp1410185.

[40] A.V. Bernatskiy, V.V. Lagunov, V.N. Ochkin, Investigation of the interaction of water molecules with the surface of a quartz tube using diode laser spectroscopy, Phys. Wave Phenom. 27 (27) (2019) 165–177, http://dx.doi.org/10.3103/S1541308X19030014.

[41] A. Schmohl, A. Miklos, P. Hess, Effects of adsorption–desorption processes on the response time and accuracy of photoacoustic detection of ammonia, Appl. Opt. 40 (15) (2001) 2571–2578, http://dx.doi.org/10.1364/AO.40.002571.

[42] Z.D. Reed, D.A. Long, H. Fleurbaey, J.T. Hodges, Si-traceable molecular transition frequency measurements at the 10−12 relative uncertainty level, Optica 7 (9) (2020) 1209–1220, http://dx.doi.org/10.1364/OPTICA.395943.

[43] R. Gamache, S. Kennedy, R. Hawkins, L. Rothman, Total internal partition sums for molecules in the terrestrial atmosphere, J. Mol. Struct. 517–518 (2000) 407–425, http://dx.doi.org/10.1016/S0022-2860(99)00266-5.

[44] R.R. Gamache, B. Vispoel, M. Rey, A. Nikitin, V. Tyuterev, O. Egorov, I.E. Gordon, V. Boudon, Total internal partition sums for the HITRAN2020 database, J. Quant. Spectrosc. Radiat. Transfer 271 (2021) (2020) 107713, http://dx.doi.org/10.1016/j.jqsrt.2021.107713.

Eugenio Fasci received his Ph.D. degree in 2011 from University of Campania Luigi Vanvitelli. He is a member of the Atoms, Molecules, and Precision Measurements group at the same University. His main scientific activities are high-precision spectroscopy of atomic and molecular species in the gas phase and development of cavity-enhanced spectroscopic methods.

Muhammad Asad Khan received his M.Sc. degree in physics from the Government College University of Lahore (Pakistan.) In 2022, as Ph. D. student, he joined the Atoms, Molecules and Precision Measurements Group at University of Campania Luigi Vanvitelli. Presently, his work is focused on Cavity Ring-Down Spectroscopy for accurate water mole fraction measurements.

Vittorio D'Agostino received his M.Sc. degree in Physics (cum laude) in 2023 from University of Campania Luigi Vanvitelli. Presently, he is a Ph.D. student at the same University, where he joined the Atoms, Molecules and Precision Measurements group.

Stefania Gravina received her Ph.D. degree in Physics in 2022 from the University of Campania. She joined the Atoms, Molecules and Precision Measurements group at the University of Campania. Her main research interests include the development of a new Doppler broadening gas thermometer based upon high-precision spectroscopy of atomic vapors as well as ultra-sensitive cavity-enhanced spectroscopy of molecular systems.

Vito Fernicola holds a degree in Physics from the University of Torino. Since 1984, he has been with INRIM, the Istituto Nazionale di Ricerca Metrologica, where he has been working in the field of thermal measurements and standards. He has been involved in the development of primary humidity standards, moisture in materials metrology, fiber optic and dielectric thermometry and instrumentation and sensors for industrial temperature and humidity measurements. He teaches Thermal Measurements and Controls at the Politecnico of Torino, where he also supervises MS and Ph.D. students in Metrology. He authored some 150 papers, many of them published in peer reviewed journals and conference proceedings, and holds four patents on novel measurement technologies.

Livio Gianfrani received his Ph.D. degree in Physics in 1993 from University of Naples Federico II. He is Professor of Physics of Matter at the Department of Mathematics and Physics of University of Campania Luigi Vanvitelli, in Caserta, where he leads the AMP

(Atoms, Molecules & Precision measurements) Group. He was guest researcher at NIST in Boulder, Colorado, in 1996/1997; guest scientist at the Center for Isotope Research of the University of Groningen, in 2002; visiting professor at the Nicolaus Copernicus University in Torun, in 2012; visiting scientist at IMRA America, Inc., Ann Arbor, in 2012; visiting professor at the Laboratoire de Physique des Lasers of the University of Sorbonne Paris Nord, in 2021. His research activities cover the field of Atomic and Molecular Physics.

Antonio Castrillo received his Ph.D. in Applied Physics in 2004 from University of Campania Luigi Vanvitelli (UniCamp) in Italy. He was a visiting researcher at the NASA AMES Research Center, USA. He is associate professor of experimental physics at UniCamp and member of the group of Atoms, Molecules and Precision measurements at the same University. His main research interest includes the development of cavity enhanced spectroscopic methods with application to high-resolution molecular spectroscopy for fundamental as well as applied physics. He authored more than 80 papers in peer-reviewed journals.